Enzyme Catalysis

DOI: 10.1002/anie.201005027

Revealing the Position of the Substrate in Nickel Superoxide Dismutase: A Model Study**

*Daniel Tietze, Stephan Voigt, Doreen Mollenhauer, Marco Tischler, Diana Imhof, Torsten Gutmann, Leticia González, Oliver Ohlenschläger, Hergen Breitzke, Matthias Görlach, and Gerd Buntkowsky**

Reactive oxygen species (ROS) are a major factor in the development of several types of cancer, inflammation, and related diseases. These ROS are not only cytotoxic but also involved in cell signaling.[1] The protection from ROS is of vital importance for biological organisms. For aerobic organisms, superoxide dismutases (SODs) play the major role in protecting cells from ROS, which are generated by the reduction of molecular oxygen by reactive metabolites of the respiratory chain.[2] Because of their biological and medical importance, SODs are a subject of intense research, which yielded more than 2000 publications in the first six months of 2010. While this research has led to detailed knowledge about their biological function and enzyme kinetics, the precise mode of action of these enzymes is still not known and two different mechanisms were proposed.[3] A major reason for this lack of knowledge is the high catalytic rate constants of superoxide degradation ($O_2^{\bullet-}$) by SODs. SODs destroy the superoxide anion radical by converting it into hydrogen peroxide and oxygen with a rate near the diffusion limit ($k_{cat} > 2\times10^9\,M^{-1}s^{-1}$).[4] Thus all transients involved in their action are too short lived to be amenable for a spectroscopic characterization. For this reason model systems of SODs were developed. Herein we show that the investigation of a model system of the nickel superoxide dismutase (NiSOD) is able to shed light into the mode of action of this enzyme and makes it possible to decide between the proposed mechanisms. In particular we are able to reveal not only the mode of binding of the substrate to the enzyme also the presence of functional water molecules in the active site of the enzyme.

Three independent classes of SODs are known. They contain either a dinuclear (Cu, Zn) or a mononuclear (Fe, Mn, Ni) cofactor.[1b,5] NiSOD, as a mononuclear nickel-containing metalloenzyme, cycles between Ni^{II} and Ni^{III} during catalysis.[3a,4b,6] NiSOD was first found in 1996 in *Streptomyces*.[5a] Crystallographic and spectroscopic studies give an impression of the structure of the whole enzyme and the geometry of its active site with a single covalently bound nickel ion. The nickel ion is embedded within the so-called nickel-hook formed by the first six amino acids of the N-terminus of the active form of *S. coelicolor* NiSOD (Scheme 1).[3a,4b,6,7]

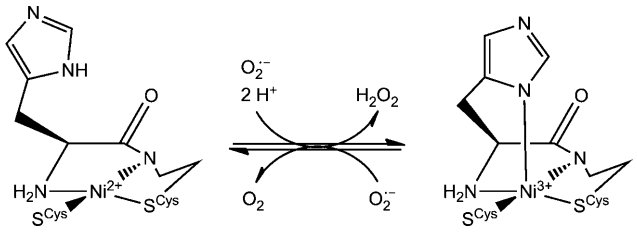

Scheme 1. Coordination geometry of NiSOD and its role in superoxide degradation.[3b]

For detailed investigations on the catalytic mechanism of the NiSOD enzyme, several catalytically active metallopeptide NiSOD models were developed based on the first 12, 9, 7, or 6 residues from the N-terminus of the active form of *S. coelicolor* NiSOD.[3b,c,8] Two mechanisms were discussed[3], which differ in the binding of the substrate. Depending on whether the substrate is bound in the first coordination sphere of the nickel ion or not they are called inner-sphere or outer-sphere electron-transfer (ET) mechanism, respectively. Recently some of us were able to synthesize and characterize a metallopeptide–substrate model complex employing cyanide as a substrate analogue. these results gave strong support for the inner-sphere ET mechanism.[9]

Studies of CuZnSODs have shown that cyanide, as a very powerful inhibitor of SODs, is ideally suited for functional studies of SODS. With CuZnSOD, cyanide forms a stable

[*] Dr. D. Tietze, Dipl.-Ing. S. Voigt, Dipl.-Chem. M. Tischler, Dr. T. Gutmann, Dr. H. Breitzke, Prof. Dr. G. Buntkowsky
Technische Universität Darmstadt, Eduard-Zintl-Institut für Anorganische und Physikalische Chemie, Petersenstrasse 22
64287 Darmstadt (Germany)
E-mail: gerd.buntkowsky@chemie.tu-darmstadt.de
Dr. D. Imhof
Friedrich-Schiller-Universität Jena
Zentrum für Molekulare Biomedizin, Institut für Biochemie
Hans-Knöll-Strasse 2, 07745 Jena (Germany)
Dipl.-Chem. D. Mollenhauer
Freie Universität Berlin, Institut für Chemie und Biochemie
Takustrasse 3, 14195 Berlin (Germany)
Prof. Dr. L. González
Friedrich- Schiller-Universität Jena, Institut für Physikalische Chemie, Helmholtzweg 4, 07743 Jena (Germany)
Dr. O. Ohlenschläger, Dr. M. Görlach
Fritz-Lipmann-Institut, Beutenbergstrasse 11
07745 Jena (Germany)

[**] The Deutsche Forschungsgemeinschaft is acknowledged for their financial support. The Fritz Lipmann Institute is financially supported by the State of Thueringia and the Federal Government of Germany.

Supporting information for this article is available on the WWW under http://dx.doi.org/10.1002/anie.201005027.

CuZnSOD-cyanide adduct, in which the cyanide is directly bound at the Cu^{2+} ion of the active site of the enzyme.[10] This complex was studied by various techniques such as EPR,[11] IR, and Raman spectroscopy,[12] crystallography,[13] and computer-based surface modeling.[14] In 2009 Shin et al. obtained crystals of an H_2O_2 complex of CuZnSOD.[15] In this complex the H_2O_2 molecule is oriented in the same way as the cyanide ligand in the cyanide-CuZnSOD-complex studied by Carugo et al.[13] Moreover the hydrogen-bond network between the CuZnSOD[14,16] and the H_2O_2 matches very well the hydrogen-bond network between the cyanide ion and the CuZnSOD.[13]

Another important feature of the NiSOD model peptides was revealed by their structure determined by 3D liquid-state NMR spectroscopy.[3b] In contrast to the *cis* configured Leu4–Pro5 peptide bond in the native enzyme, the models had a *trans* peptide bond in this position.[3b] Moreover DFT calculations indicated that the carbonyl group of the *trans* configured Leu4–Pro5 peptide bond probably adopts the role of the fifth ligand and forces substrates to approach the nickel center from the opposite side to that in the native enzyme.[3b] To shed light on the mode of action, the manner of inhibition of the enzyme by cyanide ions (discussed by Barondeau and co-workers for both the native enzyme[3a] as well as the metallopeptides[3c]), and to reveal the exact mode of binding of the cyanide ions to the enzyme, we decided to study the structure of the peptide–cyanide complex. As neither X-ray crystallography nor liquid-state NMR (L-NMR) spectroscopy are able to reveal the structure of the complex, solid-state NMR (SS-NMR) in combination with quantum chemical calculations are employed.

For this we first had to develop and analyze different ^{13}C- and ^{15}N-labeled substrate models derived from the metallopeptides of Shearer and Weston. They are based on the first seven residues from the N-terminus of the active form of *S. coelicolor* NiSOD (standard solid-phase peptide synthesis using the Fmoc strategy (Fmoc: 9-Fluorenylmethoxycarbonyl) purification with semi preparative HPLC, conversion into metallopeptides by addition of $NiCl_2$[3b,9]). These metallopeptides were labeled with a ^{13}C or ^{15}N spin label on a single position in the backbone, and were then complexed with the ^{15}N- or ^{13}C-enriched cyanide (both 98% for ^{15}N or ^{13}C, the formulas of the resulting complexes are given in Table 1).[9]

The electronic spectroscopic properties of the hepta-metallopeptide and the cyanide adduct as shown below are very similar to the nona-metallopeptide and its cyanide adduct. Moreover shortening the peptide to the presumed minimal NiSOD motif of six residues does not affect SOD activity at all.[3c] The characteristic absorption maxima of [Ni(mSOD)] and [Ni(CN)(mSOD)] at $\lambda = 458$ and 410 nm are also present in [Ni(m^7SOD)] and [Ni(CN)(m^7SOD)] (Figure 1).

As previous results indicate, cyanide binding to the metallopeptide seems to be an equilibrium reaction between the formation of the metallopeptide cyanide adduct and the $[Ni(CN)_4]^{2-}$ ion. To optimize the preparation of our solid-state NMR samples a maximum concentration of nickel-bound cyanide is needed, and this was monitored by UV/Vis spectroscopy. It is found that the concentration maximum of

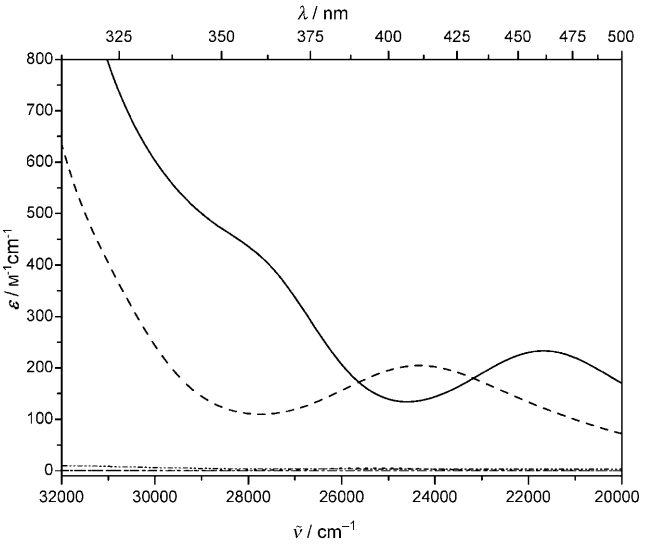

Figure 1. UV/Vis spectra of [Ni(m^7SOD)] (——), [Ni(m^7SOD)] + 2 KCN (-----), $NiCl_2$ (•••••), KCN (–•–•), and (m^7SOD) (–••–••).

the metallopeptide cyanide adduct complex is reached as soon as more than 1.6 equiv KCN are added to the solution of [Ni(m^7SOD)]. If more than 2 equiv were added the extinction coefficient at $\lambda = 410$ nm decreases in an exponential decay until 50 equiv KCN were added and the formation of $[Ni(CN)_4]^{2-}$ can be detected (further UV/Vis spectra are presented in the Supporting Information).

The distances between the labeled positions in the cyanide and in the peptide backbone were determined by means of REDOR NMR spectroscopy. With this method the magnetic heteronuclear dipolar coupling between two nuclei can be determined, the strength of which is proportional to r^{-3} (where r = the distance between two dipolar coupled spins). In this way the binding of azide to the human MnSOD has been successfully studied.[17] However, to employ this method an adequate molecular structure is needed. As no suitable molecular structure of a NiSOD substrate model exists we determined the 3D structure of our NiSOD substrate model by means of liquid-state NMR spectroscopy. Since, we applied standard two-dimensional proton-correlated NMR experiments to assign the resonances for the unlabeled [Ni(CN)(m^7SOD)], we obtained no structural information about the nickel-bound cyanide ion.[3c,19]

The resulting [Ni(CN)(m^7SOD)] structure superimposes well with a reported NiSOD biomimetic which does not have an attached substrate analogue (standard deviation for residues His1–Cys6 0.57 Å).[3c] A similar result was found for the CuZnSOD cyanide adduct. Also in that system the cyanide coordinating at the copper ion has only a very minor influence on the local structure of the active site and in particular does not change the number of amino acid ligands on copper ion in the active site.[10,11,14,15] Again, proline-5 has a *trans* peptide bond. The aromatic ring of the N-terminal His1 residue did not contribute to the well-defined nickel-binding region (for more details, see Supporting Information).

The REDOR NMR spectroscopic study of the five different singly isotope labeled cyanide-NiSOD complexes

(Table 1) gave values for the interaction between the spin labels. These were used to model the cyanide ion manually into the liquid NMR structure to give the structure shown in Figure 2. This structure shows the cyanide ion is bound to the nickel ion as postulated by Barondeau et al.[3a] and Herbst et al.[20]

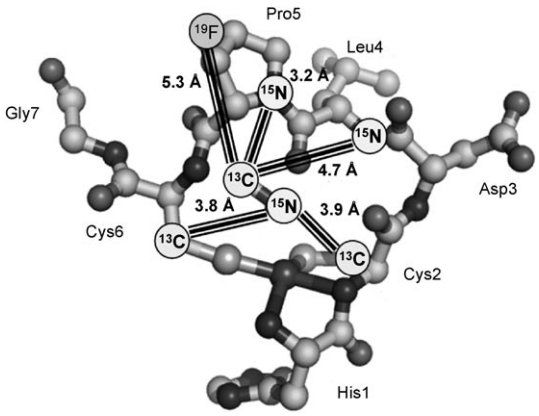

Figure 2. The liquid NMR structure of the peptide backbone of the cyanide adduct. The labeled positions and the distances derived from REDOR measurements are also shown.

To support the experimental structural evaluation, quantum chemical structure optimizations of the cyanide-based complex were performed. In a first step only the cyanide anion was modeled into the peptide. The obtained structures were compared to the experimental data of the liquid NMR structure and the REDOR measurements. Structure **A** shows best agreement with experimental data (Figure 3). The

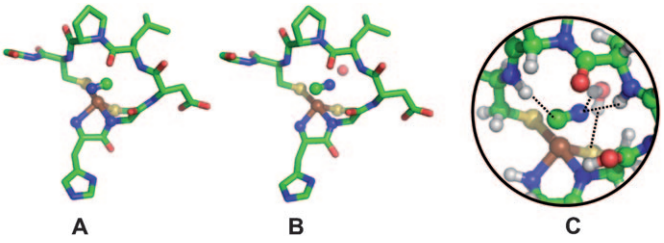

Figure 3. Optimized structures at the BP86(MARI-J; COSMO)/TZVP level of theory (**A** and **B**). The nickel ion, the cyanide anion, and the coordinated atoms are in ball and stick representation; hydrogen atoms are not shown. **A**: Structure optimized without water; **B**: Structure model **A** optimized with one water molecule; **C**: Enlargement of structure **B**, including hydrogen atoms; hydrogen bonds to the cyanide anion are shown as dotted lines. Colors as in Scheme 2.

relevant bond lengths are given in Table 1. The cyanide anion coordinates through its triple bond to the nickel(II) center. The resulting complex has a trigonal-bipyramidal coordination geometry. In the second step an additional water molecule was added to the active site. The optimized structure **B** (Figure 3) reveals an inverted orientation of the cyanide compared to the waterless structure **A**, and has a much better agreement with the distances determined by REDOR (Table 1; RMS = 0.67).

Table 1: Experimental REDOR distances for complexes **a**–**e** and the distances derived from the optimized structures **A** and **B** from Figure 3 and root mean square (RMS) deviation. All distances are given in Å.

Peptides[a]	CN^- to	Exp.	**A**	**B**
[Ni($C^{15}N$)(m^7SOD-$^{13}C_\beta$-Cys2)] **a**	C^β (Cys2)	3.9 ± 0.3	4.3	3.3
[Ni($C^{15}N$)(m^7SOD-$^{13}C_\beta$-Cys6)] **b**	C^β (Cys6)	3.8 ± 0.1	3.4	4.0
[Ni(^{13}CN)(m^7SOD-^{15}N-Leu)] **c**	N^α (Leu)	4.7 ± 0.4	3.1	3.9
[Ni(^{13}CN)(m^7SOD-ProF)] **d**	$H(F)^\gamma$ (Pro)	5.3 ± 0.2	6.7	6.7
[Ni(^{13}CN)(mSOD-^{15}N-Pro)] **e**	N^α (Pro)	3.2 ± 0.2	3.7	3.8
RMS			1.02	0.67

[a] mSOD: H-HCDLPCGVY-NH_2; m^7SOD: H-HCDLPCG-NH_2.

Furthermore, the position of the water molecule and the cyanide ion in structure **B** resemble those of the chloride ion in the active site of the recently published crystal structure of an Y9F-NiSOD mutant[20] (PDB entry 1T6U). In that mutant, Tyr9 was replaced by a Phe, causing an anion binding site to open enabling an halogen anion (Cl^- or Br^-) to bind above the Ni^{II} center giving a very similar bonding situation to that in **B**.[20]

The water molecule in **B** has two hydrogen bonds, one to the nitrogen atom of the cyanide ion and the other to the sulfur of the Cys2 residue (see **C** in Figure 3). The cyanide is stabilized by hydrogen bonds to the amide protons of Leu5 and Cys6. Therefore we conclude that the water molecule seems to play a stabilizing role for the cyanide anion. In light of all the hydrogen bonds, the cyanide anion appears to be fixed within the peptide environment.

The hydrogen-bond network, especially with the water molecule, would also explain the broad solid-state ^{15}N-NMR cyanide signals observed earlier by us and during the solid-state NMR measurements (mainly for the REDOR experiments) for this work.

A similar result was found for the cyanide ion in the cyanide adduct of CuZnSOD. The cyanide is embedded within a hydrogen-bond network and directly bound to the copper ion.[13] Furthermore, this copper-bound cyanide precisely matches the position and orientation of H_2O_2 in the active site of CuZnSOD as revealed from the crystal structure of a H_2O_2 complex of CuZnSOD.[13,15]

For CuZnSOD the hydrogen-bond network stabilizes the substrate in the active site environment and is essential to promote electron transfer between the substrate and the metal center.[14–16] Based on their DFT calculations Carloni et al. concluded that a functional water molecule acts as a proton source for superoxide conversion in CuZnSOD.[16a] Furthermore, they found that superoxide should be able to displace the copper-bound water molecule from the active site. Finally the superoxide is oxidized to molecular oxygen, which is displaced by a water molecule.[15,16a]

The water molecule is present in the crystal structure of the wild type NiSOD enzyme and the Y9F-NiSOD mutant, hence we assume it also plays an important role for the catalytic degradation of the superoxide for the NiSOD enzyme as well as for the NiSOD-active metallopeptides. Therefore, this water molecule is presumed to be the source for the protons which are necessary for $O_2^{\bullet-}$ degradation, as is the case in CuZnSOD. Thus, our results clearly indicate a

strong similarity between the catalytic mechanism of NiSOD and CuZnSOD. Moreover the similar behavior of the two isoenzymes despite their differences in both the primary structure and their cofactors is a clear indication of the importance of this water molecule for the biological function of the enzymes. Our results could therefore be useful in determining the mode of action of other superoxide dismutases.

In 2004 Barondeau et al. postulated a first catalytic cycle for the NiSOD enzyme.[3a] In their model, the superoxide coordinates above the plane of the quadratic-planar coordination environment at the active site of the NiSOD enzyme while the His1-imidazole side chain can coordinate from the opposite side of the nickel ion forming an trigonal-pyramidal (Structure II in Scheme 2) or an octahedral (Structure IV, in Scheme 2) transition state. Our experimental data clearly

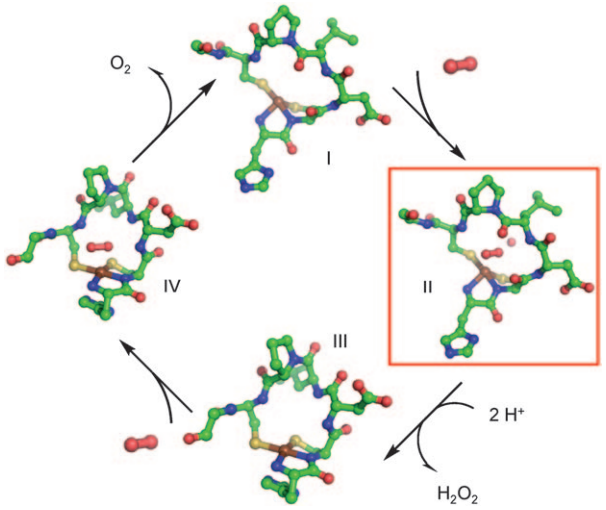

Scheme 2. Proposed catalytic cycle for the superoxide degradation in the NiSOD. Ni^{III} oxidation state is found in the bound His-imodazole ring complex (Structures III and IV), while Ni^{II} oxidation state is in the unbound His-imodazole-ring complex (structures I and II). The framed structure represents the DFT optimized structure II of our metallopeptide cyanide adduct. Here the calculations revealed the presence of a functional water molecule (pink sphere) in the active center, which is probably the proton source of the reaction. The other structures which are used to illustrate the mode of action of the NiSOD are only schematic. Ni Brown, O red, N blue, S yellow.

corroborate this model. They indicate that the cyanide ion in the metallopeptide cyanide adduct is located at the position proposed by Barondeau et al for the substrate,[3a] and that the cyanide ion is directly bound to the Ni^{II} center Combining our DFT calculations and NMR measurements, it is evident that at least one of the protons required for the generation of H_2O_2 (II–IV in Scheme 2) is provided by a water molecule in the active site. Thus is possible to propose the catalytic cycle in Scheme 2

We have developed a peptide-based model system of the enzyme-substrate complex of the NiSOD. The structure of this peptide model matches closely the structure of the relevant part of the native enzyme. The combination of NMR spectroscopy and quantum-chemical calculations reveals, for the first time, the position of the substrate of NiSOD. The resulting position of the substrate analogue strongly supports the reaction mechanism postulated by Barondeau et al.,[3a] of a directly nickel-bound substrate. Furthermore the role of structural water molecules in the functioning of the enzymes is revealed and allows us to propose an improved catalytic cycle for superoxide degradation. Finally, the manner of inhibition of NiSOD by cyanide ions is unraveled, the cyanide ion coordinates at the nickel center and blocks the coordination site for the natural substrate.

Experimental Section

Solid-state NMR measurements were carried out on a Bruker Avance II^+ spectrometer at 400 MHz proton frequency utilizing a Bruker 3.2 mm HFXY probe under MAS conditions and various spinning rates. CP-MAS sequences as well as 90° single pulse were employed. The ^{13}C spectra are referenced to TMS and ^{15}N spectra are referenced to $CH_3{}^{15}NO_2$. The ^{19}F spectrum is referenced to F-apatite. REDOR NMR measurements were carried out using a ^{13}C or ^{15}N (98% enriched) or ^{19}F backbone-labeled 7mer/9mer metallopeptide with ^{13}C, ^{15}N (98% enriched) labeled cyanide as substrate. The measured dipolar couplings were converted into internuclear distances by the help of a self-prepared MATLAB script. Sample preparation and measurements: All samples were prepared from freeze dried powder (complex **e** was diluted in a 1:4 ratio with unlabeled material). The data points of the REDOR measurements were smoothed (**a**–**d**: 2-point FFT smoothing, **e**: 6-point adjacent averaging smoothing) and fitted by a literature procedure.[21] Solution structure NMR experiments were performed on Bruker Avance III spectrometers with proton frequencies of 600 MHz or 750 MHz. Freeze-dried samples of metallopeptide cyanide powder were dissolved in 90% H_2O/10% D_2O (pH 7.8 adjusted with 0.1M NaOH). Data were acquired and processed with Topspin (Bruker, Rheinstetten, Germany) and analyzed with XEASY.[22] The proton resonance assignment was performed by using a combination of 2D [^{1}H,^{1}H]-DQF-COSY,[^{1}H,^{1}H]-TOCSY (60 ms spinlock time) and [^{1}H,^{1}H]-ROESY experiments. ROESY experiments were acquired with 100 and 120 ms mixing time. In addition, a natural abundance [^{1}H,^{13}C]-HSQC spectrum was acquired. Distance constraints were extracted from a 2D [^{1}H,^{1}H]-ROESY spectrum. Upper limit distance constraints were calibrated according to their intensity in the ROESY spectrum.

UV/Vis measurements were recorded on a Varian Cary 5000 UV/Vis-NIR spectrophotometer using quartz cuvettes with 1 cm pathlength. All solutions were prepared from doubly distilled water at pH 7.8.

Further details of the REDOR measurements the solution structure determination of the metallopeptide cyanide adduct, computational details of the structure optimization, and a description of the peptide synthesis and UV/Vis data can be found in the Supporting Information.

Received: August 11, 2010
Revised: November 16, 2010
Published online: February 25, 2011

Keywords: density functional calculations · enzyme catalysis · solid-state NMR spectroscopy · substrate binding · superoxide dismutase

[1] a) J. J. Haddad, *Cell. Signalling* **2002**, *14*, 879 – 897; b) J. M. Mates, J. M. Segura, C. Perez-Gomez, R. Rosado, L. Olalla, M. Blanca, F. M. Sanchez-Jimenez, *Blood Cells Mol. Dis.* **1999**, *25*, 103 – 109.

[2] J. S. Valentine, D. L. Wertz, T. J. Lyons, L.-L. Liou, J. J. Goto, E. B. Gralla, *Curr. Opin. Chem. Biol.* **1998**, *2*, 253 – 262.

[3] a) D. P. Barondeau, C. J. Kassmann, C. K. Bruns, J. A. Tainer, E. D. Getzoff, *Biochemistry* **2004**, *43*, 8038 – 8047; b) K. P. Neupane, K. Gearty, A. Francis, J. Shearer, *J. Am. Chem. Soc.* **2007**, *129*, 14605 – 14618 ; c) M. Schmidt, S. Zahn, M. Carella, O. Ohlenschläger, M. Görlach, E. Kothe, J. Weston, *ChemBioChem* **2008**, *9*, 2135 – 2146.

[4] a) P. A. Bryngelson, S. E. Arobo, J. L. Pinkham, D. E. Cabelli, M. J. Maroney, *J. Am. Chem. Soc.* **2004**, *126*, 460 – 461; b) S. B. Choudhury, J. W. Lee, G. Davidson, Y. I. Yim, K. Bose, M. L. Sharma, S. O. Kang, D. E. Cabelli, M. J. Maroney, *Biochemistry* **1999**, *38*, 3744 – 3752; c) M. Cox, D. Nelson, A. Lehninger in *Lehninger Biochemie*, *Vol. 3*, Springer, Heidelberg, **2001**.

[5] a) T. Eitinger, *J. Bacteriol.* **2004**, *186*, 7821 – 7825 ; b) A. Schmidt, G. Haferburg, E. Kothe, *J. Basic Microbiol.* **2007**, *47*, 56 – 62; c) H. D. Youn, E. J. Kim, J. H. Roe, Y. C. Hah, S. O. Kang, *Biochem. J.* **1996**, *318*, 889 – 896.

[6] J. Wuerges, J. W. Lee, Y. I. Yim, H. S. Yim, S. O. Kang, K. D. Carugo, *Proc. Natl. Acad. Sci. USA* **2004**, *101*, 8569 – 8574.

[7] a) A. T. Fiedler, P. A. Bryngelson, M. J. Maroney, T. C. Brunold, *J. Am. Chem. Soc.* **2005**, *127*, 5449; b) T. A. Jackson, T. C. Brunold, *Acc. Chem. Res.* **2004**, *37*, 461; c) J. Wuerges, J. W. Lee, S. O. Kang, K. D. Carugo, *Acta Crystallogr. Sect. D* **2002**, *58*, 1220.

[8] a) K. P. Neupane, J. Shearer, *Inorg. Chem.* **2006**, *45*, 10552; b) M. Schmidt, Friedrich-Schiller-Universität Jena, **2007**; c) J. Shearer, A. Dehestani, F. Abanda, *Inorg. Chem.* **2008**, *47*, 2649; d) J. Shearer, L. M. Long, *Inorg. Chem.* **2006**, *45*, 2358; e) J. Shearer, N. F. Zhao, *Inorg. Chem.* **2006**, *45*, 9637.

[9] D. Tietze, H. Breitzke, D. Imhof, E. Kothe, J. Weston, G. Buntkowsky, *Chem. Eur. J.* **2009**, *15*, 517 – 523.

[10] G. Rotilio, Finazzia. A, Calabres. L, F. Bossa, Guerrier. P, B. Mondovi, *Biochemistry* **1971**, *10*, 616 – 621.

[11] a) J. A. Fee, J. Peisach, W. B. Mims, *J. Biol. Chem.* **1981**, *256*, 1910 – 1914; b) G. Rotilio, B. Mondovi, L. Morpurgo, L. Calabres, C. Giovagno, *Biochemistry* **1972**, *11*, 2187 – 2192; c) H. L. Van Camp, R. H. Sands, J. A. Fee, *Biochim. Biophys. Acta Protein Struct. Mol. Enzymol.* **1982**, *704*, 75 – 89.

[12] J. Han, N. J. Blackburn, T. M. Loehr, *Inorg. Chem.* **1992**, *31*, 3223 – 3229.

[13] K. D. Carugo, A. Battistoni, M. T. Carri, F. Polticelli, A. Desideri, G. Rotilio, A. Coda, M. Bolognesi, *FEBS Lett.* **1994**, *349*, 93 – 98.

[14] J. A. Tainer, E. D. Getzoff, J. S. Richardson, D. C. Richardson, *Nature* **1983**, *306*, 284 – 287.

[15] D. S. Shin, M. DiDonato, D. P. Barondeau, G. L. Hura, C. Hitomi, J. A. Berglund, E. D. Getzoff, S. C. Cary, J. A. Tainer, *J. Mol. Biol.* **2009**, *385*, 1534 – 1555.

[16] a) P. Carloni, P. E. Bloechl, M. Parrinello, *J. Phys. Chem.* **1995**, *99*, 1338 – 1348; b) M. Rosi, A. Sgamellotti, F. Tarantelli, I. Bertini, C. Luchinat, *Inorg. Chem.* **1986**, *25*, 1005 – 1008.

[17] a) T. Gullion, *Concepts Magn. Reson.* **1998**, *10*, 277 – 289; b) T. Gullion, J. Schaefer, *J. Magn. Reson.* **1989**, *81*, 196 – 200; c) D. D. Laws, H. M. L. Bitter, A. Jerschow, *Angew. Chem.* **2002**, *114*, 3224; *Angew. Chem. Int. Ed.* **2002**, *41*, 3096.

[18] T. Emmler, I. Ayala, D. Silverman, S. Hafner, A. S. Galstyan, E. W. Knapp, G. Buntkowsky, *Solid State Nucl. Magn. Reson.* **2008**, *34*, 6 – 13.

[19] K. Wüthrich, *NMR of Proteins and Nucleic Acids*, Wiley, New York, **1986**.

[20] R. W. Herbst, A. Guce, P. A. Bryngelson, K. A. Higgins, K. C. Ryan, D. E. Cabelli, S. C. Garman, M. J. Maroney, *Biochemistry* **2009**, *48*, 3354 – 3369.

[21] K. T. Mueller, *J. Magn. Reson. Ser. A* **1995**, *113*, 81 – 93.

[22] C. Bartels, T. H. Xia, M. Billeter, P. Guntert, K. Wüthrich, *J. Biomol. NMR* **1995**, *6*, 1 – 10.

